



Xu Wang · Ping Yang · Peter Schiavone 

A screw dislocation interacting with a semi-infinite crack partially penetrating a parabolic elastic inhomogeneity

Received: 20 August 2020 / Accepted: 8 October 2020 / Published online: 17 November 2020
© Springer-Verlag GmbH Austria, part of Springer Nature 2020

Abstract We consider the interaction of a screw dislocation with a semi-infinite crack partially penetrating a parabolic elastic inhomogeneity embedded in an infinite elastic matrix subjected to anti-plane mechanical loading. Analytical solutions are derived in the case when the screw dislocation is located either in the matrix or inside the parabolic inhomogeneity. In addition, the local mode III stress intensity factor at the crack tip and the image force acting on the screw dislocation are obtained and illustrated accordingly. Moreover, we establish a dislocation emission criterion from the crack.

1 Introduction

The shielding of cracks owing to the presence of nearby dislocations has been discussed by many investigators (see, for example, [1–10]). The dislocation–crack interaction problem becomes considerably challenging when the tip of the crack is lodged inside an elastic inhomogeneity. In this case, the dislocation interacts not only with the crack, but also with the elastic inhomogeneity.

In this paper, we investigate the interaction between a screw dislocation and a semi-infinite crack partially penetrating a parabolic elastic inhomogeneity under far-field anti-plane mechanical loading. The crack passes through the vertex of the parabolic interface and has its tip located at the focus of the parabolic interface. Under this assumption, analytical solutions are derived for two specific cases: (i) when the screw dislocation is located in the matrix; (ii) when the screw dislocation is located inside the parabolic elastic inhomogeneity. In addition, the local mode III stress intensity factor at the crack tip and the image force acting on the screw dislocation are obtained. The shielding effect of the screw dislocation on the local mode III stress intensity factor is illustrated for typical locations of the screw dislocation. The condition for dislocation emission from the crack is established.

2 General solution

As shown in Fig. 1, we consider a semi-infinite crack with its cleavage plane on the negative x_1 -axis partially penetrating a parabolic elastic inhomogeneity. Let S_1 , S_2 , and S_3 denote, respectively, the upper half matrix,

X. Wang (✉) · P. Yang
School of Mechanical and Power Engineering, East China University of Science and Technology, 130 Meilong Road, Shanghai 200237, China
E-mail: xuwang@ecust.edu.cn

P. Schiavone (✉)
Department of Mechanical Engineering, University of Alberta, 10-203 Donadeo Innovation Centre for Engineering, Edmonton, Alberta, Canada
E-mail: p.schiavone@ualberta.ca

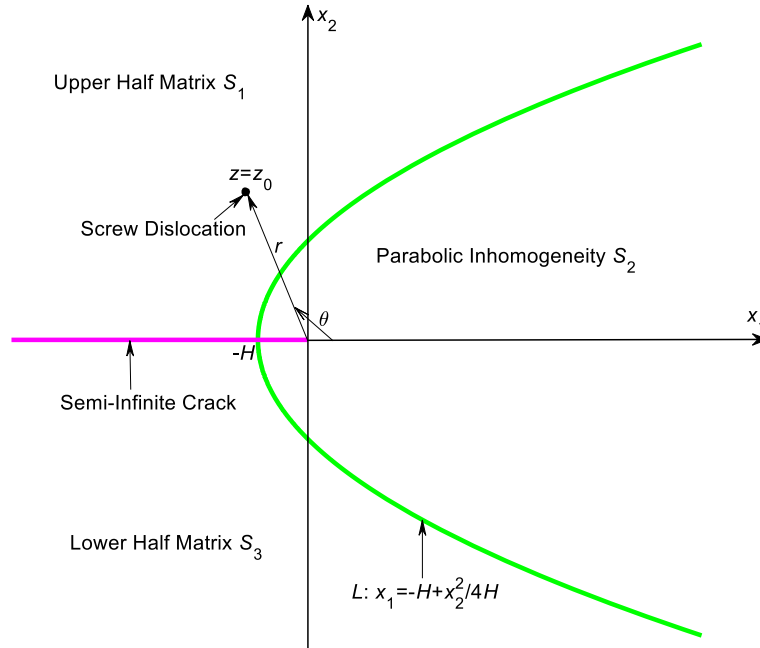


Fig. 1 A screw dislocation interacting with a semi-infinite crack partially penetrating a parabolic elastic inhomogeneity

the inhomogeneity, and the lower half matrix, all of which are perfectly bonded through the parabolic interface L described by

$$L : x_1 = -H + \frac{x_2^2}{4H}, \quad H > 0. \quad (1)$$

The crack passes through the vertex of the parabolic interface at $z = -H$, and the crack tip is located at the focus of the parabola L . In addition, a screw dislocation with Burgers vector b is applied at $z = z_0 = r \exp(i\theta)$ with r and θ being the polar coordinates of z_0 either in the upper half matrix S_1 or in the inhomogeneity S_2 . Throughout the paper, the subscripts 1, 2, and 3 are used to identify the respective quantities in S_1 , S_2 , and S_3 .

For the anti-plane shear deformations of an isotropic elastic material, the two anti-plane shear stress components σ_{31} and σ_{32} , the out-of-plane displacement u_3 , and the single stress function ϕ can be expressed in terms of a single analytic function $f(z)$ of the complex variable $z = x_1 + ix_2$ as [11]

$$\sigma_{32} + i\sigma_{31} = \mu f'(z), \quad \phi + i\mu u_3 = \mu f(z), \quad (2)$$

where μ is the shear modulus. In addition, the two anti-plane stress components can be expressed in terms of the single stress function by [11]

$$\sigma_{32} = \phi_{,1}, \quad \sigma_{31} = -\phi_{,2}. \quad (3)$$

We introduce the following conformal mapping function:

$$z = \omega(\xi) = \xi^2, \quad \xi = \omega^{-1}(z) = \sqrt{z}, \quad \text{Re}\{\xi\} \geq 0. \quad (4)$$

As shown in Fig. 2, using the mapping function in Eq. (4), the z -plane containing the semi-infinite crack is mapped onto the right half-plane: $\text{Re}\{\xi\} \geq 0$; the upper half matrix S_1 is mapped onto the upper and right quarter-plane $S'_1 : \{h \leq \text{Im}\{\xi\} < +\infty, \text{Re}\{\xi\} \geq 0\}$ with $h = \sqrt{H}$; the parabolic inhomogeneity S_2 is mapped onto the middle semi-infinite strip $S'_2 : \{-h \leq \text{Im}\{\xi\} \leq h, \text{Re}\{\xi\} \geq 0\}$; the lower half matrix S_3 is mapped onto the lower and right quarter-plane $S'_3 : \{-\infty < \text{Im}\{\xi\} \leq -h, \text{Re}\{\xi\} \geq 0\}$; the crack surfaces are mapped onto the vertical straight line: $\{\text{Re}\{\xi\} = 0, -\infty < \text{Im}\{\xi\} < +\infty\}$; the location of the screw dislocation at $z = z_0$ is mapped onto the point $\xi = \xi_0$ with $\xi_0 = \sqrt{z_0}$.

By imposing the continuity conditions of traction and displacement across the perfect parabolic interface L , all three analytic functions $f_i(\xi) = f_i(\omega(\xi))$, $i = 1, 2, 3$ can be expressed in terms of a single analytic function $g(\xi)$ as follows:

$$f_3(\xi) = g(\xi),$$

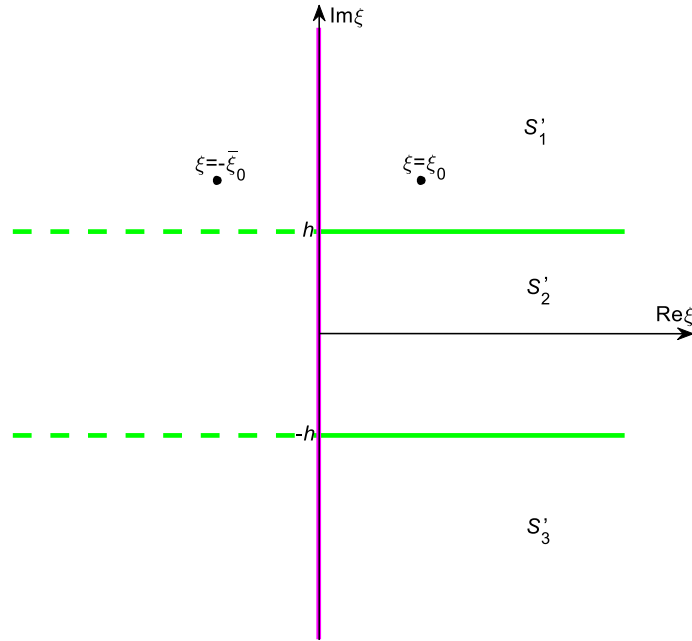


Fig. 2 The image ξ -plane

$$\begin{aligned}
 f_2(\xi) &= \frac{\Gamma + 1}{2} g(\xi) + \frac{\Gamma - 1}{2} \bar{g}(\xi + 2ih), \\
 f_1(\xi) &= \frac{(\Gamma + 1)^2}{4\Gamma} g(\xi) - \frac{(\Gamma - 1)^2}{4\Gamma} g(\xi - 4ih) \\
 &\quad + \frac{\Gamma^2 - 1}{4\Gamma} \bar{g}(\xi + 2ih) - \frac{\Gamma^2 - 1}{4\Gamma} \bar{g}(\xi - 2ih),
 \end{aligned} \tag{5}$$

where

$$\Gamma = \frac{\mu_1}{\mu_2}. \tag{6}$$

It remains to determine the specific expression for $g(\xi)$. Once $g(\xi)$ is known, the three analytic functions $f_1(\xi)$, $f_2(\xi)$, and $f_3(\xi)$ can be conveniently determined using Eq. (5).

3 Screw dislocation in S_1

When the screw dislocation is located in the upper half matrix S_1 , the analytic function $g(\xi)$ is given by

$$g(\xi) = \sqrt{\frac{2}{\pi}} \frac{K_{III}}{\mu_1} \xi + \frac{2b\Gamma}{\pi(\Gamma + 1)^2} \sum_{n=0}^{+\infty} M^{2n} \ln(\xi - \xi_0 - 4nhi) - \frac{2b\Gamma}{\pi(\Gamma + 1)^2} \sum_{n=0}^{+\infty} M^{2n} \ln(\xi + \bar{\xi}_0 - 4nhi), \tag{7}$$

where K_{III} is the mode III intensity factor characterizing the far-field loading, and

$$M = \frac{\Gamma - 1}{\Gamma + 1}, \quad |M| < 1. \tag{8}$$

Substitution of Eq. (7) into Eq. (5) yields the following explicit expressions for $f_1(\xi)$, $f_2(\xi)$, and $f_3(\xi)$:

$$\begin{aligned}
 f_3(\xi) &= \sqrt{\frac{2}{\pi}} \frac{K_{III}}{\mu_1} \xi + \frac{2b\Gamma}{\pi(\Gamma + 1)^2} \sum_{n=0}^{+\infty} M^{2n} \ln(\xi - \xi_0 - 4nhi) \\
 &\quad - \frac{2b\Gamma}{\pi(\Gamma + 1)^2} \sum_{n=0}^{+\infty} M^{2n} \ln(\xi + \bar{\xi}_0 - 4nhi),
 \end{aligned} \tag{9.1}$$

$$\begin{aligned}
f_2(\xi) = & \sqrt{\frac{2}{\pi}} \frac{K_{\text{III}}}{\mu_2} \xi + \frac{b\Gamma}{\pi(\Gamma+1)} \sum_{n=0}^{+\infty} M^{2n} \ln(\xi - \xi_0 - 4nhi) \\
& - \frac{b\Gamma}{\pi(\Gamma+1)} \sum_{n=0}^{+\infty} M^{2n} \ln(\xi + \bar{\xi}_0 - 4nhi) \\
& + \frac{b\Gamma}{\pi(\Gamma+1)} \sum_{n=0}^{+\infty} M^{2n+1} \ln[\xi - \bar{\xi}_0 + 2(2n+1)hi] \\
& - \frac{b\Gamma}{\pi(\Gamma+1)} \sum_{n=0}^{+\infty} M^{2n+1} \ln[\xi + \xi_0 + 2(2n+1)hi],
\end{aligned} \tag{9.2}$$

$$\begin{aligned}
f_1(\xi) = & \sqrt{\frac{2}{\pi}} \frac{K_{\text{III}}}{\mu_1} \xi \\
& + \frac{b}{2\pi} \ln(\xi - \xi_0) - \frac{b}{2\pi} \ln(\xi + \bar{\xi}_0) \\
& + \frac{b}{2\pi} \sum_{n=0}^{+\infty} M^{2n+1} \ln[\xi - \bar{\xi}_0 + 2(2n+1)hi] - \frac{b}{2\pi} \sum_{n=0}^{+\infty} M^{2n+1} \ln[\xi + \xi_0 + 2(2n+1)hi] \\
& - \frac{b}{2\pi} \sum_{n=0}^{+\infty} M^{2n+1} \ln[\xi - \bar{\xi}_0 + 2(2n-1)hi] + \frac{b}{2\pi} \sum_{n=0}^{+\infty} M^{2n+1} \ln[\xi + \xi_0 + 2(2n-1)hi].
\end{aligned} \tag{9.3}$$

The local mode III stress intensity factor, denoted here by k_{III} , can be derived from $f_2(\xi)$ in Eq. (9.2) as follows:

$$k_{\text{III}} = K_{\text{III}} - \sqrt{\frac{2}{\pi}} \frac{b\mu_1}{\Gamma+1} \sqrt{r} \cos \frac{\theta}{2} \sum_{n=0}^{+\infty} \frac{M^n}{r + 4n\sqrt{Hr} \sin \frac{\theta}{2} + 4n^2 H}. \tag{10}$$

Using $f_1(\xi)$ in Eq. (9.3) and the Peach–Koehler formula [12], the image force acting on the screw dislocation is then

$$\begin{aligned}
F_1 - iF_2 = & \frac{K_{\text{III}}b}{\sqrt{2\pi}\xi_0} - \frac{\mu_1 b^2}{8\pi\xi_0^2} - \frac{\mu_1 b^2}{4\pi\xi_0} \left(\frac{1}{\xi_0 + \bar{\xi}_0} + \frac{M}{\xi_0 - \bar{\xi}_0 - 2hi} - \frac{M}{2\xi_0 - 2hi} \right) \\
& + \frac{\mu_1 b^2(1-M^2)(\xi_0 + \bar{\xi}_0)}{8\pi\xi_0} \sum_{n=0}^{+\infty} \frac{M^{2n+1}}{[\xi_0 + (2n+1)hi][\xi_0 - \bar{\xi}_0 + 2(2n+1)hi]},
\end{aligned} \tag{11}$$

where F_1 and F_2 are, respectively, the force components along the x_1 and x_2 directions. It can be easily verified that when $M = 0$, Eqs. (10) and (11) simply reduce to the classical solution by Majumdar and Burns [1].

4 Screw dislocation in S_2

When the screw dislocation is located within the parabolic inhomogeneity S_2 , the analytic function $g(\xi)$ is given by

$$\begin{aligned}
g(\xi) = & \sqrt{\frac{2}{\pi}} \frac{K_{\text{III}}}{\mu_1} \xi + \frac{b}{\pi(\Gamma+1)} \sum_{n=0}^{+\infty} M^{2n} \ln(\xi - \xi_0 - 4nhi) \\
& + \frac{b}{\pi(\Gamma+1)} \sum_{n=0}^{+\infty} M^{2n+1} \ln[\xi - \bar{\xi}_0 - 2(2n+1)hi] \\
& - \frac{b}{\pi(\Gamma+1)} \sum_{n=0}^{+\infty} M^{2n} \ln(\xi + \bar{\xi}_0 - 4nhi) - \frac{b}{\pi(\Gamma+1)} \sum_{n=0}^{+\infty} M^{2n+1} \ln[\xi + \xi_0 - 2(2n+1)hi].
\end{aligned} \tag{12}$$

Substitution of Eq. (12) into Eq. (5) yields the following explicit expressions for $f_1(\xi)$, $f_2(\xi)$, and $f_3(\xi)$:

$$\begin{aligned} f_3(\xi) = & \sqrt{\frac{2}{\pi}} \frac{K_{\text{III}}}{\mu_1} \xi + \frac{b}{\pi(\Gamma+1)} \sum_{n=0}^{+\infty} M^{2n} \ln(\xi - \xi_0 - 4nhi) \\ & + \frac{b}{\pi(\Gamma+1)} \sum_{n=0}^{+\infty} M^{2n+1} \ln[\xi - \bar{\xi}_0 - 2(2n+1)hi] \\ & - \frac{b}{\pi(\Gamma+1)} \sum_{n=0}^{+\infty} M^{2n} \ln(\xi + \bar{\xi}_0 - 4nhi) - \frac{b}{\pi(\Gamma+1)} \sum_{n=0}^{+\infty} M^{2n+1} \ln[\xi + \xi_0 - 2(2n+1)hi], \end{aligned} \quad (13.1)$$

$$\begin{aligned} f_2(\xi) = & \sqrt{\frac{2}{\pi}} \frac{K_{\text{III}}}{\mu_2} \xi + \frac{b}{2\pi} \sum_{n=0}^{+\infty} M^{2n} \ln(\xi - \xi_0 - 4nhi) + \frac{b}{2\pi} \sum_{n=0}^{+\infty} M^{2n+1} \ln[\xi - \bar{\xi}_0 - 2(2n+1)hi] \\ & - \frac{b}{2\pi} \sum_{n=0}^{+\infty} M^{2n} \ln(\xi + \bar{\xi}_0 - 4nhi) - \frac{b}{2\pi} \sum_{n=0}^{+\infty} M^{2n+1} \ln[\xi + \xi_0 - 2(2n+1)hi] \\ & + \frac{b}{2\pi} \sum_{n=0}^{+\infty} M^{2n+1} \ln[\xi - \bar{\xi}_0 + 2(2n+1)hi] + \frac{b}{2\pi} \sum_{n=0}^{+\infty} M^{2n+2} \ln[\xi - \xi_0 + 4(n+1)hi] \\ & - \frac{b}{2\pi} \sum_{n=0}^{+\infty} M^{2n+1} \ln(\xi + \xi_0 + 2(2n+1)hi) - \frac{b}{2\pi} \sum_{n=0}^{+\infty} M^{2n+2} \ln[\xi + \bar{\xi}_0 + 4(n+1)hi], \end{aligned} \quad (13.2)$$

$$\begin{aligned} f_1(\xi) = & \sqrt{\frac{2}{\pi}} \frac{K_{\text{III}}}{\mu_1} \xi + \frac{b(\Gamma+1)}{4\pi\Gamma} \ln(\xi - \xi_0) - \frac{b(\Gamma+1)}{4\pi\Gamma} \ln(\xi + \bar{\xi}_0) \\ & + \frac{b(\Gamma-1)}{4\pi\Gamma} \sum_{n=0}^{+\infty} M^{2n} \ln[\xi - \bar{\xi}_0 + 2(2n+1)hi] + \frac{b(\Gamma-1)}{4\pi\Gamma} \sum_{n=0}^{+\infty} M^{2n+1} \ln[\xi - \xi_0 + 4ih(n+1)] \\ & - \frac{b(\Gamma-1)}{4\pi\Gamma} \sum_{n=0}^{+\infty} M^{2n} \ln[\xi + \xi_0 + 2(2n+1)hi] - \frac{b(\Gamma-1)}{4\pi\Gamma} \sum_{n=0}^{+\infty} M^{2n+1} \ln[\xi + \bar{\xi}_0 + 4ih(n+1)] \\ & - \frac{b(\Gamma-1)}{4\pi\Gamma} \sum_{n=1}^{+\infty} M^{2n} \ln[\xi - \bar{\xi}_0 + 2(2n-1)hi] - \frac{b(\Gamma-1)}{4\pi\Gamma} \sum_{n=0}^{+\infty} M^{2n+1} \ln(\xi - \xi_0 + 4nhi) \\ & + \frac{b(\Gamma-1)}{4\pi\Gamma} \sum_{n=1}^{+\infty} M^{2n} \ln[\xi + \xi_0 + 2(2n-1)hi] + \frac{b(\Gamma-1)}{4\pi\Gamma} \sum_{n=0}^{+\infty} M^{2n+1} \ln(\xi + \bar{\xi}_0 + 4nhi). \end{aligned} \quad (13.3)$$

The local mode III stress intensity factor can be derived from $f_2(\xi)$ in Eq. (13.2) as follows:

$$k_{\text{III}} = K_{\text{III}} - \frac{\mu_2 b}{\sqrt{2\pi}} \sqrt{r} \cos \frac{\theta}{2} \left(\sum_{n=0}^{+\infty} \frac{M^n}{r + 4n\sqrt{Hr} \sin \frac{\theta}{2} + 4n^2 H} + \sum_{n=1}^{+\infty} \frac{M^n}{r - 4n\sqrt{Hr} \sin \frac{\theta}{2} + 4n^2 H} \right), \quad (14)$$

Using $f_2(\xi)$ in Eq. (13.2) and the Peach–Koehler formula, the image force acting on the screw dislocation is given by

$$\begin{aligned} F_1 - iF_2 = & \frac{K_{\text{III}} b}{\sqrt{2\pi} \xi_0} - \frac{\mu_2 b^2}{8\pi \xi_0^2} - \frac{\mu_2 b^2}{4\pi \xi_0 (\xi_0 + \bar{\xi}_0)} - \frac{\mu_2 b^2 (\xi_0 + \bar{\xi}_0)}{2\pi \xi_0} \sum_{n=1}^{+\infty} \frac{M^{2n}}{(\xi_0 + \bar{\xi}_0)^2 + 16n^2 h^2} \\ & + \frac{\mu_2 b^2 (\xi_0 - \bar{\xi}_0)}{2\pi \xi_0} \sum_{n=0}^{+\infty} \frac{M^{2n+1}}{(\xi_0 - \bar{\xi}_0)^2 + 4(2n+1)^2 h^2} - \frac{\mu_2 b^2}{4\pi} \sum_{n=0}^{+\infty} \frac{M^{2n+1}}{\xi_0^2 + (2n+1)^2 h^2}. \end{aligned} \quad (15)$$

It is again not difficult to verify that when $M = 0$, Eqs. (14) and (15) simply reduce to the classical solution by Majumdar and Burns [1].

5 Discussion

In this section, several typical cases will be discussed in detail to demonstrate the analytical solutions obtained in the previous two sections and to establish a dislocation emission criterion from the crack.

5.1 The screw dislocation is absent

In the absence of the screw dislocation with $b = 0$, it is seen from Eqs. (9.1–3) and (13.1–3) that

$$\begin{aligned} f_1(z) = f_3(z) &= \sqrt{\frac{2}{\pi}} \frac{K_{\text{III}}}{\mu_1} \sqrt{z}, \quad z \in S_1 \cup S_3; \\ f_2(z) &= \sqrt{\frac{2}{\pi}} \frac{K_{\text{III}}}{\mu_2} \sqrt{z}, \quad z \in S_2, \end{aligned} \quad (16)$$

which indicates that the stress field in the two-phase composite: $\sigma_{32} + i\sigma_{31} = K_{\text{III}}/\sqrt{2\pi z}$, $z \in S_1 \cup S_2 \cup S_3$ is identical to that near the tip of a mode III crack. In this case, $k_{\text{III}} \equiv K_{\text{III}}$, which is in sharp contrast to the analogous result for a semi-infinite crack partially penetrating a circular elastic inhomogeneity [13].

5.2 A screw dislocation far from the crack tip

When the screw dislocation is located far from the crack tip (i.e., $r \rightarrow \infty$), both Eqs. (10) and (14) reveal that

$$k_{\text{III}} \cong K_{\text{III}} - \frac{\mu_1 b}{\sqrt{2\pi r}} \cos \frac{\theta}{2}, \quad r \rightarrow \infty, \quad (17)$$

and Eq. (11) for a screw dislocation in the upper half matrix becomes

$$F_1 - iF_2 \cong \frac{K_{\text{III}} b}{\sqrt{2\pi} \xi_0} - \frac{\mu_1 b^2}{8\pi \xi_0^2} - \frac{\mu_1 b^2}{4\pi \xi_0 (\xi_0 + \bar{\xi}_0)}, \quad r \rightarrow \infty, \quad (18)$$

and Eq. (15) for a screw dislocation inside the parabolic inhomogeneity becomes

$$F_1 - iF_2 \cong \frac{K_{\text{III}} b}{\sqrt{2\pi r}} - \frac{b^2(\mu_1 + \mu_2)}{8\pi r}, \quad r \rightarrow \infty \text{ and } \theta \rightarrow 0. \quad (19)$$

Equations (17) and (18) are the corresponding equations for a screw dislocation near a semi-infinite crack in a homogeneously elastic plane with shear modulus μ_1 [1]. The result in Eqs. (17) and (18) implies that when the screw dislocation in the matrix is located far from the crack tip, the interaction problem can be treated equivalently to the case when the z -plane is elastically homogeneous with shear modulus μ_1 .

5.3 A screw dislocation on the parabola L

When the screw dislocation is located on the parabola L , the following relationship is established: $\sqrt{r} \sin \frac{\theta}{2} = \sqrt{H}$. In this case, it follows from either Eq. (10) or Eq. (14) that

$$k_{\text{III}} = K_{\text{III}} - \frac{\mu_1 b Y(r)}{\sqrt{2\pi r}} \cos \frac{\theta}{2}, \quad (20)$$

where the function $Y(r)$ is defined as

$$Y(r) = r(1 - M) \sum_{n=0}^{+\infty} \frac{M^n}{r + 4Hn(n+1)} > 0, \quad r \geq H, \quad (21)$$

which is illustrated in Fig. 3 for different values of M . It is seen from Fig. 3 that: $0 < Y(r) < 1$ when $M > 0$; $Y(r) \equiv 1$ when $M = 0$; $Y(r) > 1$ when $M < 0$. The shielding effect of the screw dislocation on the local mode III stress intensity factor can be clearly observed from Fig. 3.

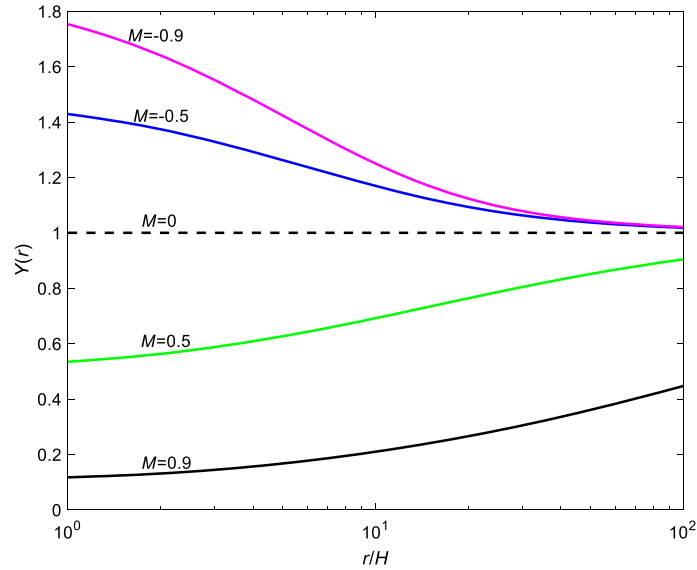


Fig. 3 Variation of the function $Y(r)$ defined by Eq. (21) for different values of M

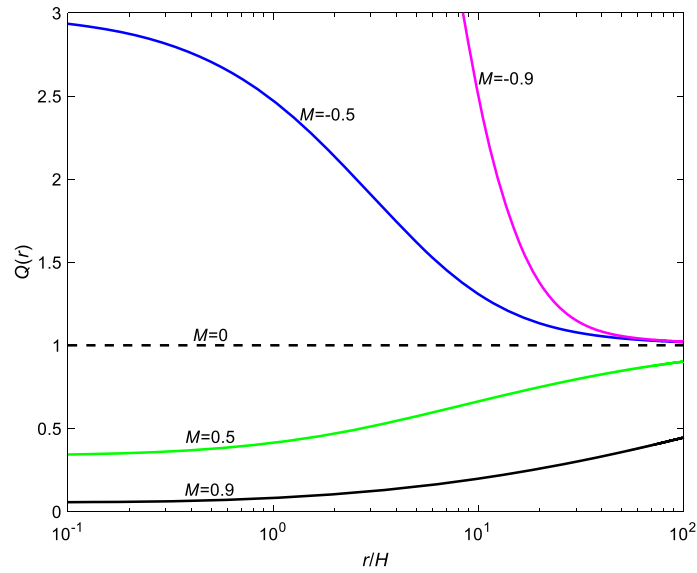


Fig. 4 Variation of the function $Q(r)$ defined by Eq. (23) for different values of M

5.4 A screw dislocation on the positive x_1 -axis inside the parabolic inhomogeneity

When the screw dislocation lies on the positive x_1 -axis inside the parabolic inhomogeneity, Eq. (14) becomes

$$k_{III} = K_{III} - \frac{\mu_1 b Q(r)}{\sqrt{2\pi r}}, \tag{22}$$

where the function $Q(r)$ is defined as

$$Q(r) = \frac{1 - M}{1 + M} \left(2r \sum_{n=0}^{+\infty} \frac{M^n}{r + 4n^2 H} - 1 \right) > 0, r \geq 0, \tag{23}$$

which is illustrated in Fig. 4 for different values of M . It is seen from Fig. 4 that the behavior of the function $Q(r)$ is quite similar to that of $Y(r)$ shown in Fig. 3. The shielding effect of the screw dislocation on the local mode III stress intensity factor is again clearly observed this time from Fig. 4.

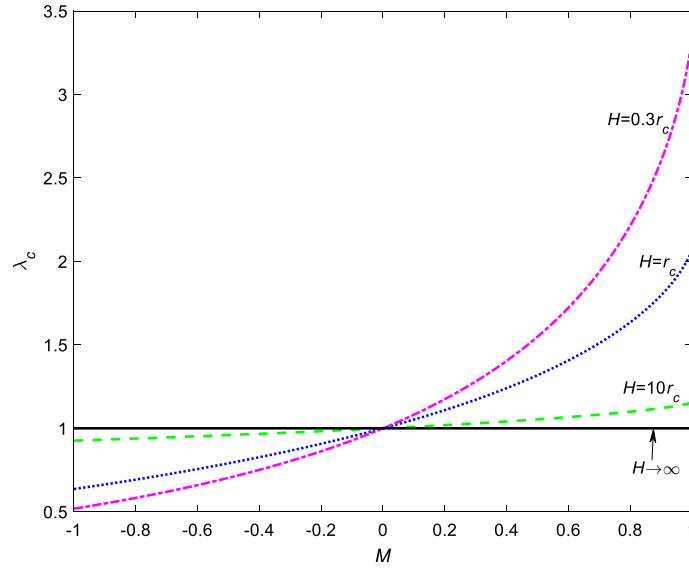


Fig. 5 Variation of λ_c defined by Eq. (26) as a function of M for different values of \tilde{H}

In addition, when the screw dislocation lies on the positive x_1 -axis inside the parabolic inhomogeneity, Eq. (15) becomes

$$F_1 = \frac{K_{\text{III}} b}{\sqrt{2\pi r}} - \frac{\mu_2 b^2}{4\pi} \sum_{n=0}^{+\infty} \frac{M^n}{r + n^2 H}, \quad F_2 = 0. \quad (24)$$

Thus, according to Rice and Thomson [14], the dislocation emission criterion from the crack can be established as follows:

$$K_{\text{III}} > K_c = \frac{\mu_2 b}{2\sqrt{2\pi r_c}} \sum_{n=0}^{+\infty} \frac{M^n}{n^2 \tilde{H} + 1}, \quad (25)$$

where $\tilde{H} = H/r_c$ in which r_c denotes the core radius of the screw dislocation and K_c is the critical stress intensity factor for dislocation emission. Illustrated in Fig. 5 is the normalized critical stress intensity factor defined by

$$\lambda_c = \frac{2\sqrt{2\pi r_c}}{\mu_2 b} K_c, \quad (26)$$

as a function of the parameter M for different values of \tilde{H} . It is seen from Fig. 5 that: (i) $0 < \lambda_c < 1$ when the inhomogeneity is harder than the matrix with $M < 0$, $\lambda_c > 1$ when the inhomogeneity is softer than the matrix with $M > 0$; (ii) λ_c is an increasing function of M , an increasing function of \tilde{H} for $M < 0$, and a decreasing function of \tilde{H} for $M > 0$.

6 Conclusions

We have analytically solved the anti-plane problem associated with a screw dislocation near a semi-infinite crack partially penetrating a parabolic elastic inhomogeneity. The general solution in terms of the single analytic function $g(\xi)$ is derived in Eq. (5). When the screw dislocation is located in the upper half matrix, the three analytic functions are given explicitly by Eqs. (9.1–3), and the local mode III stress intensity factor and the image force are, respectively, presented in Eqs. (10) and (11). When the screw dislocation lies inside the parabolic inhomogeneity, the three analytic functions are given explicitly by Eqs. (13.1–3), and the local mode III stress intensity factor and the image force are presented in Eqs. (14) and (15), respectively.

Acknowledgements This work is supported by the National Natural Science Foundation of China (Grant No. 11272121) and by a Discovery Grant from the Natural Sciences and Engineering Research Council of Canada (Grant No: RGPIN-2017-03716115112).

References

1. Majumdar, B.S., Burns, S.J.: Crack tip shielding - an elastic theory of dislocations and dislocation arrays near a sharp crack. *Acta Metall.* **29**, 579–588 (1981)
2. Ohr, S.M., Chang, S.J., Thomson, R.: Elastic interaction of a wedge crack with a screw dislocation. *J. Appl. Phys.* **57**, 1839–1843 (1985)
3. Lin, I.H., Thomson, R.: Cleavage, dislocation emission and shielding for cracks under general loading. *Acta Metall.* **34**, 187–206 (1986)
4. Zhang, T.Y., Li, J.C.M.: Image forces and shielding effects of an edge dislocation near a finite length crack. *Acta Metall. Mater.* **39**, 2739–2744 (1991)
5. Lee, K.Y., Lee, W.G., Pak, Y.E.: Interaction between a semi-infinite crack and a screw dislocation in a piezoelectric material. *ASME J. Appl. Mech.* **67**, 165–170 (2000)
6. Huang, M.X., Li, Z.H.: Dislocation emission criterion from a blunt crack tip. *J. Mech. Phys. Solids* **52**, 1991–2003 (2004)
7. Bhandakkar, T.K., Chng, A.C., Curtin, W.A., Gao, H.: Dislocation shielding of a cohesive crack. *J. Mech. Phys. Solids* **58**, 530–541 (2010)
8. Wang, X., Fan, H.: Interaction between a nanocrack with surface elasticity and a screw dislocation. *Math. Mech. Solids* **22**(2), 131–143 (2017)
9. Wang, X., Schiavone, P.: Interaction between a completely coated semi-infinite crack and a screw dislocation. *Z. angew. Math. Phys.* **70**(4), 116 (2019)
10. Wang, X., Schiavone, P.: An edge dislocation interacting with two semi-infinite cracks. *Eng. Fract. Mech.* **232**, 107044 (2020)
11. Ting, T.C.T.: *Anisotropic Elasticity-Theory and Applications*. Oxford University Press, New York (1996)
12. Dundurs, J.: Elastic interaction of dislocations with inhomogeneities. In: Mura, T. (ed.) *Mathematical Theory of Dislocations*, pp. 70–115. American Society of Mechanical Engineers, New York (1969)
13. Steif, P.S.: A semi-infinite crack partially penetrating a circular inclusion. *ASME J. Appl. Mech.* **54**, 87–92 (1987)
14. Rice, J.R., Thomson, R.: Ductile versus brittle behaviour of crystals. *Philos. Mag.* **29**, 73–97 (1974)

Publisher's Note Springer Nature remains neutral with regard to jurisdictional claims in published maps and institutional affiliations.